# A Classical Trajectory Study of $O^- + HF \rightarrow OH + F^-$

**Stephanie Lau and Sally Chapman***

*Department of Chemistry, Barnard College, Columbia University, New York, New York 10027−6598*

*Received: August 20, 1996; In Final Form: December 9, 1996*[⊗]

Quasiclassical trajectories have been used to investigate the heavy−light−heavy ion−molecule reaction, $O^- + HF \rightarrow OH + F^-$, using approximate potential energy surfaces. Multiple surface effects are neglected. 1D and 3D dynamics on the same surface produce very different vibrational distributions. OH product vibrational distributions are relatively insensitive to details of the potential. Product rotational energy distributions, on the other hand, are quite sensitive to features of the potential surface, particularly the steepness of the bend. Long-range ion−dipole forces play an important role in the dynamics, particularly in the angular distributions. Product vibrational energy and angular distributions are compared to two sets of experiments.

## I. Introduction

The fundamental process of proton transfer has been studied extensively in both the gas and liquid phase. Several experimental techniques have been utilized to explore the detailed gas-phase dynamics, including flow tubes,[1,2] ion emission,[3,4] laser-induced fluorescence,[5,6] and molecular beams.[7,8] Some of these studies have focused on proton transfer between halogens: $X^- + HY \rightarrow HX + Y^-$. An interesting observation in these systems[3,4] was the similarity of the product state distributions with those of the analogous neutral hydrogen transfer reactions, $X + HY \rightarrow HX + Y$. Because halogen atoms have similar electron affinities, the asymptotic energetics in the corresponding reactions are similar, but the intervening surfaces are clearly very different: the ionic reactions pass through a deep hydrogen-bonded well, while the neutral systems pass over a barrier. It has been argued that the special kinematics of heavy−light−heavy reactions are responsible for the similar dynamics.[3] A collinear classical trajectory study[9] lent some support to this hypothesis.

Heavy−light−heavy reactions, the focus of extensive theoretical attention,[10−22] exhibit interesting characteristic dynamics. There have been many studies of collinear symmetric halogen-containing systems.[10−18] The kinematics of this mass combination gives rise to a wide disparity in the time scales for motion of the heavy and light particles. Hyperspherical coordinates (polar when collinear) are particularly revealing, since for these systems the hyperradius $\rho$ is effectively the heavy particle (X−Y) coordinate. Because motion in the heavy and light particle coordinates is nearly separable, these systems are often called *vibrationally adiabatic*. Models exploiting this adiabaticity[13−16] offer powerful insights, for example giving a clear explanation of the rich resonance structure in the reaction probabilities. Studies of three-dimensional systems[18−22] have demonstrated that sharp features in collinear results are often averaged out in the full dynamics, although this can depend on the details of the potential surface.[21] In a review article, Skodje[18] emphasized the important role played by rotation in 3D heavy−light−heavy dynamics.

Two groups have carried out experiments giving detailed dynamical information on a somewhat different gas-phase proton transfer reaction: $O^- + HF \rightarrow OH + F^-$. Leone and co-workers,[5,6] using a flow−drift tube, studied the effect of collision energy on product vibrational excitation of the OH product at thermal to moderate collision energies (3.8, 9.6, and 15.4 kJ/mol). They found that the OH($\nu'$=1) population increases linearly with available energy above threshold, a result at variance with the expectation of vibrational adiabaticity. Farrar and co-workers[7,8] studied the same reaction in a crossed molecular beam apparatus at higher collision energies (40.5, 45.0, and 55.8 kJ/mol). They observed substantial (but not entirely symmetric) forward−backward peaking in the reactive angular distribution, with an interesting subtle difference in the angular distribution for the different OH($v'$) states. Although these higher energy vibrational excitations exceed those seen in the drift tube experiments, the collision energy dependence is no longer linear. These interesting results suggested that a trajectory study might be illuminating.

## II. The Potential Energy Surface

Collinear $OHF^-$ is a $^2\Pi$ molecule. Thus the $O^- + HF$ reaction is properly governed by a pair of potential energy surfaces which are nearly degenerate for collinear geometries (degenerate in the absence of spin−orbit coupling). The degeneracy is lifted when the molecule bends. For simplicity, however, we will model this as a single-surface problem.

Little information is available about the $OHF^-$ surface. Bradforth *et al.*,[23] whose experiments probed the spectroscopy of the transition state of neutral OHF by photodetaching an electron from the anion, carried out *ab initio* (Hartree−Fock and second-order Møller−Plesset) studies of the anion. They calculated that $OHF^-$ is linear with distances $r_{OH} = 1.078$ Å (2.037 $a_0$) and $r_{HF} = 1.346$ Å (2.543 $a_0$), and with well depth 193.7 kJ/mol below the reactants. The surface is exoergic by 52.5 kJ/mol (these energies exclude zero-point vibration). The stretching frequencies calculated at the minimum were 433 and 2015 $cm^{-1}$, corresponding to [24] valence force constants $k_{11} = 0.260$, $k_{12} = 0.093$, and $k_{22} = 0.069$ au. Reference 23 also includes a plot of a slice of the collinear potential surface through the well at fixed $r_{HF}$.

This information, combined with known properties of the asymptotic molecules, was used in devising a collinear potential energy surface. The potential function $V(r_1,r_2,r_3)$ was developed previously to describe the ground state singlet surface for bihalide ions: $XHY^-$ (with X and Y halogens). This semiempirical function is based on a very simple two-state $2 \times 2$ diatomics-in-molecules (DIM) approach[25] to describe the $^1\Sigma$ states of the linear $XHY^-$ molecule. The two DIM states correlate with the following atoms

[⊗] Abstract published in *Advance ACS Abstracts,* February 15, 1997.

S1089-5639(96)02555-8 CCC: $14.00 

$$\alpha: \quad X^-(^1S) + H(^2S) + Y(^2P)$$

$$\beta: \quad X(^2P) + H(^2S) + Y^-(^1S)$$

The relevant diatomic states formed from basis α are $HX^-$ ($^2\Sigma$), HY ($^1\Sigma$), and $XY^-$ ($^2\Sigma$) and those from basis $\beta$ are HX ($^1\Sigma$), $HY^-$ ($^2\Sigma$), and $XY^-$ ($^2\Sigma$). Coupling between α and $\beta$ is caused by the interaction of the two $XY^-$ diabatic states. Labeling the distances 1 = HX, 2 = HY, and 3 = XY, the potential $V^{DIM}$ is given by the lower eigenvalue of the following 2 × 2 matrix:

$$H_{\alpha\alpha} = E_1(r_1) + M_2(r_2) + M_3(r_3) - EA(X)$$

$$H_{\beta\beta} = M_1(r_1) + E_2(r_2) + M_3(r_3) - EA(Y)$$

$$H_{\alpha\beta} = E_3(r_3) \qquad (1)$$

$EA(Z)$ is the electron affinity of $Z$. $M_i$ is a Morse function for the ground state of the diatomic molecule $i$. Spectroscopic Morse parameters are used for $M_1$ and $M_2$.

In principle, $M_3$ and $E_3$ are diabatic functions which give rise to the two $^2\Sigma$ states of the $XY^-$ molecule ($^2\Sigma_g$ and $^2\Sigma_u$ for $X_2^-$). In practice, this very small DIM is not predictive, so these terms, along with $E_1$ and $E_2$, are treated as empirical functions whose parameters are varied to give a satisfactory fit. The functions $E_i$ are exponentials ($Ae^{-br}$). This potential was used previously for $FHF^-$, $ClHCl^-$, and $FHCl^-$.[18] The use of the same function for $OHF^-$ is not theoretically motivated but is simply for convenience. Like the well-known extended LEPS (London−Eyring−Polanyi−Sato) potential,[26] this function incorporates correct asymptotic information, leaving a few parameters free for fitting. Unlike the LEPS function, the two asymptotes may dissociate to different atomic states, a feature useful for asymmetric ion−molecule systems.

The parameters for the initial collinear $OHF^-$ were obtained by a least squares fit to points near the well, based on the calculations of Bradforth *et al.*[23] The resulting function has a minimum, 194.9 kJ/mol below the reactants, at $r_{OH} = 2.031$ $a_0$ and $r_{HF} = 2.504$ $a_0$. Parameters and features of the potential are in Table 1. The fit to Bradforth's data, shown in Table 2, is approximate, but the surface has reasonable qualitative features. A contour map is shown in Figure 1.

The information used to generate this collinear surface is limited to the region near the deep well. In order to examine possible dynamical effects of the features of the surface away from the well, in particular in the corner where $r_{OH}$ and $r_{HF}$ are both small, a term was added, producing two modified surfaces designated II and III:

$$V^{wall} = A_w \exp(-b_w r_3) \qquad (2)$$

Parameters were chosen so $V^{wall}$ has a minor effect on the surface at the $OHF^-$ minimum: the geometry and force constants are essentially unchanged. However it increases the steepness of the repulsive wall where trajectories turn the corner at short $r_{HF}$ and $r_{OH}$. Parameters (in atomic units) for this term are as follows: surface I, $A_w = 0$; surface II, $A_w = 37\,750$, $b_w = 4$; surface III, $A_w = 1.0 \times 10^{16}$, $b_w = 9.8$.

Two modifications to the potential were made for 3D dynamical studies. The first introduces correct long-range ion−dipole forces. This change is less important for 1D dynamics, since it simply adds a longer range tail to an already attractive surface. However, proper asymptotic behavior is important in three-dimensional dynamics for two reasons: first, the anisotropy of the ion−dipole interaction ($V = \mu_D \cos\theta/R^2$) may orient the approaching reactants, and second, reaction cross sections are strongly sensitive to the long-range forces.

**TABLE 1: Collinear Surface Parameters (Atomic Units)**

| function | parameter | OH | HF | OF |
|---|---|---|---|---|
| Morse ($M$) | $D_e$ | 0.169 817 | 0.225 | 0.001 49 |
| | $r_e$ | 1.834 51 | 1.732 88 | 8.85 |
| | $\beta$ | 1.215 57 | 1.174 03 | 0.36 |
| exponential ($E$) | $A$ | 7.01 | 13.6 | 0.877 |
| | $b$ | 1.33 | 2.57 | 0.266 |
| electron affinities | O | 0.053 837 3 | F | 0.124 91 |

**TABLE 2: Potential at the OHF Minimum**

| | Bradforth *et al.*[a] | this work |
|---|---|---|
| $r_1 = r_{OH}$ (au) | 2.037 | 2.031 |
| $r_2 = r_{HF}$ (au) | 2.544 | 2.503 |
| $V$ (kJ/mol) below $O^- + HF$ | −193.7 | −194.9 |
| $k_{11}$ (au) | 0.260[b] | 0.217 |
| $k_{12}$ (au) | 0.093[b] | 0.085 |
| $k_{22}$ (au) | 0.069[b] | 0.061 |
| $\omega_1$ ($cm^{-1}$) | 433 | 398 |
| $\omega_3$ ($cm^{-1}$) | 2015 | 1768 |

[a] Reference 23 except as noted. [b] Reference 24.

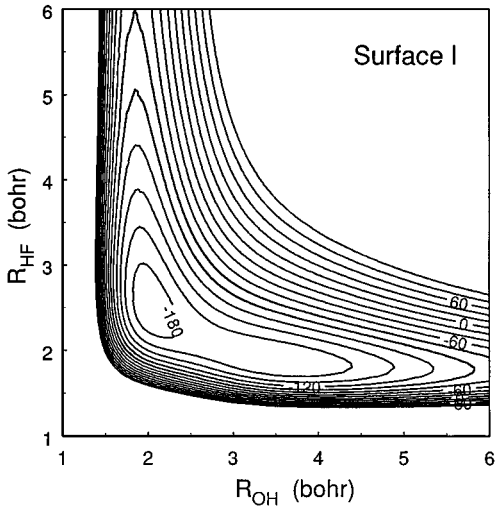


**Figure 1.** Contour map of collinear surface I. Contours are at 20 kJ/mol intervals. Energies are measured from separated reactants.

The modified potential is

$$V = V^{SR}(1 - S_1)(1 - S_2) + V_1^{LR}S_1 + V_2^{LR}S_2 \qquad (3)$$

where $V^{SR} = V^{DIM} + V^{wall} + V^{bend}$ ($V^{bend}$ is defined below). $V_k^{LR}$ gives the long-range ion−dipole potential in the entrance (1 = $O^- + HF$) and exit (2 = $OH + F^-$) channels (with the diatomic described by a Morse):

$$V_1^{LR} = Q_1(1/r_3 - 1/r_1) + M_2(r_2)$$

$$V_2^{LR} = Q_2(1/r_3 - 1/r_2) + M_1(r_1) + \Delta E \qquad (4)$$

$Q_1 = \mu_{HF}/r_{HF}^0 = 0.41457$ au and $Q_2 = \mu_{OH}/r_{OH}^0 = 0.357698$ au. $\mu_i$ are dipole moments, $r_i^0$ are the equilibrium bond distances, and $\Delta E$ is the exoergicity of the surface. The switch $S$ is a hyperbolic tangent:

$$S_i = {}^1/_2\{1 + \tanh(c(r_i - r_i^X)\} \qquad (5)$$

$r_i^X$ is set at the approximate crossing point of the $V^{LR}$ and $V^{SR}$ curves along the collinear reaction path ($r_1^X = 9.75$, $r_2^X = 6.00$ au). The parameter $c$ (2.0 for both channels) was chosen to

produce a smooth connection. No new long-range surface minima are introduced by the $V^{LR}$ terms.

A second modification influences the bending behavior of the short-range potential. Without this term, surfaces I−III above favor noncollinear geometries. To remedy this, we add the following term, which vanishes for collinear geometries:

$$V^{\text{bend}} = \left(\frac{1}{r_1 + r_2} - \frac{1}{r_3}\right)\left(\frac{A_1}{r_1} + \frac{A_2}{r_2} + \frac{A_3}{r_3^2}\right) \qquad (6)$$

$A_1$ and $A_2$ were chosen so that the anisotropies [$(V(\text{X}-\text{YH}) - V(\text{X}-\text{HY})$] of the long- and short-range potentials match on the minimum energy path at the midpoint of the switch $S_k$ ($A_1 = 0.85$, $A_2 = 1.95$ au). Even with $A_3 = 0$, this term produces a surface which favors collinear geometries. Surfaces I−III, with $A_3 = 0$, have a bending force constant at the $OHF^-$ minimum of 0.0317 au. Nonzero values of $A_3$ further modify the steepness of the bend. Surface IV (identical to surface I when collinear) has $A_3 = 10$ au, producing a bending force constant (0.0582 au) equal to the average of the two calculated by Bradforth *et al.*[23] [Collinear $OHF^-$, a $^2\Pi$ molecule, has different bending frequencies (1064 and 1225 $cm^{-1}$) perpendicular and parallel to the partially filled $\pi$ orbital.] The harmonic bending frequency for surfaces I−III is 817 $cm^{-1}$ and for surface IV is 1110 $cm^{-1}$.

## III. Collinear Dynamics

There are several reasons why collinear dynamics may provide an inadequate picture for this system. First, while the minimum energy path is collinear, it passes through a deep minimum on the potential energy surface, so a wide range of bent geometries is energetically accessible even for the lowest energy collisions. Second, the large thermal rate constant for this reaction[5] implies that large-impact parameter collisions play an important role. Finally, as noted above, previous work[18] on neutral heavy−light−heavy systems indicates that rotation is often important. However, since collinear models continue to play an important role in the understanding of the dynamics of heavy−light−heavy systems, it seemed worthwhile to examine briefly 1D dynamics and to compare it with 3D dynamics for this system.

Quasiclassical trajectories were used, with collision energies which spanned the two sets of experiments. Product vibrational excitations are compared with the experiment in Figure 2. The agreement between surface I and experiment is poor: this surface produces much too much vibrational excitation of the OH product. To see what features of the potential are important in producing this result, it is useful to compare the role of *direct* and *complex* trajectories. For simplicity, a direct trajectory is defined as one which has a single turning point in the heavy atom separation $r_{OF}$. About a third to a half of the reactive collisions were direct for surface I; direct reactions correlate with significantly lower product vibration. Thus reducing complex formation should decrease $E_v$(OH). Surfaces II and III, with a steeper wall in the corner of the potential, were designed for this purpose. These surfaces produce significantly larger fractions of direct collisions, and both result in less product vibrational excitation.

On surface I, as the collision energy increases, the *fraction* of available energy deposited into OH vibration is roughly constant (about 75%; since we are using classical dynamics, reactant zero-point vibration is counted as available here). On surfaces II and III, the *amount* of energy channeled into OH vibration is roughly constant (about 40 kJ/mol). In other words, on surface I, excess translational energy is partially converted to product vibration, while on surfaces II and III, it is channeled into translation. The latter is more characteristic of vibrationally adiabatic behavior, where the heavy particle (translational) coordinate is only weakly coupled to the light particle (vibrational) coordinate. It is not surprising that increasing the probability of direct collisions enhances adiabaticity.

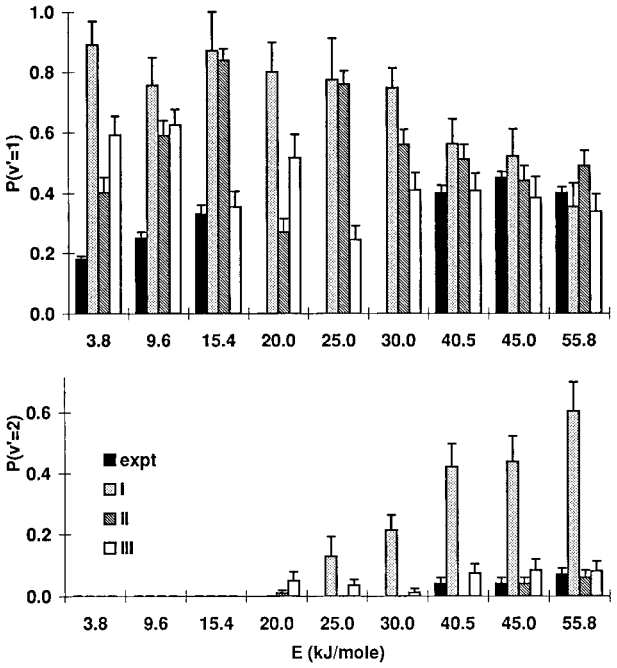


**Figure 2.** Probability of forming OH in $v = 1$ and $v = 2$: experiments (refs 6−8) and collinear trajectory results on three surfaces. Error bars on trajectory results represent 1 standard deviation in the statistics.

Surfaces II and III give product vibrational distributions roughly comparable to experiment at the higher energies, but the agreement remains unsatisfactory at lower collision energies. While it is possible that further collinear surface modification might improve this, we did not pursue this further.

## IV. 3D Dynamics

Quasiclassical trajectories were used to study the 3D dynamics on surfaces I, II, and IV. Batches of 1000 or more trajectories were run for each set of initial conditions. Most runs had HF($v$=0,$J$=0). A collision was characterized as direct if the hyperradius ($\rho^2 = \mu R^2 + mr^2$) had a single turning point. Some properties were tallied separately for direct events. All calculations were done on PC computers (486-DX66). Table 3 gives a summary of results.

Total reactive cross sections are shown in Figure 3. The long-range forces lead to very large cross sections, particularly at lower energies. The energy dependence of the cross section is similar to the capture cross section for a locked dipole[27]

$$\sigma(E) = \pi q \mu_D / E + \pi q (2\alpha/E)^{1/2}$$

where $\mu_D$ is the dipole moment and $\alpha$ the polarizability of HF. The second term is the familiar Langevin cross section. This agreement is in part fortuitous: the potential used for the trajectories does not have an ion-induced dipole $r^{-4}$ term but has stronger shorter range attractions. The trajectory value for $b_{max}$, the maximum impact parameter for reactive trajectories, corresponds to that for a simple locked dipole [$b_{max} = (\mu_D/E)^2$] only at the lowest energy, where about half the collisions are nonreactive. At higher energies, the maximum impact parameters are a bit larger than the simple dipole prediction. The corresponding maximum orbital angular momenta are large:

**TABLE 3: Selected Average Product Properties**

| $E_T$[a] | $\sigma$[b] | %$C$[c] | $\langle E_v\rangle$[d] | $\Delta$[e] | $\langle E_R\rangle$ | $\Delta$ | $\langle E_T\rangle$ | $\Delta$ | $\langle\chi\rangle$[f] |
|---|---|---|---|---|---|---|---|---|---|
| | | | | Surface I: HF($v$=0,$J$=0) | | | | | |
| 3.8 | 1242 ± 20 | 95 | 22.5 | 16.1 | 15.1 | 13.4 | 32.4 | 16.2 | 90.2 |
| 9.6 | 649 ± 13 | 89 | 23.6 | 17.1 | 13.6 | 13.4 | 38.7 | 18.0 | 92.2 |
| 15.4 | 511 ± 11 | 86 | 24.6 | 18.3 | 14.0 | 15.9 | 43.1 | 20.5 | 91.9 |
| 20.0 | 418 ± 9 | 80 | 25.7 | 18.5 | 12.2 | 15.2 | 48.4 | 20.9 | 89.9 |
| 25.0 | 357 ± 8 | 78 | 27.7 | 19.0 | 13.2 | 15.9 | 50.4 | 21.6 | 89.6 |
| 30.0 | 299 ± 7 | 75 | 28.6 | 19.7 | 13.4 | 17.2 | 54.4 | 23.3 | 89.7 |
| 40.5 | 207 ± 6 | 67 | 30.8 | 20.7 | 14.0 | 17.5 | 62.0 | 25.0 | 88.4 |
| 45.0 | 164 ± 6 | 66 | 32.1 | 22.4 | 13.5 | 18.3 | 65.7 | 26.4 | 83.6 |
| 55.8 | 132 ± 5 | 68 | 35.4 | 25.2 | 17.9 | 21.9 | 68.8 | 30.3 | 80.7 |
| | | | | Surface I: HF($v$=0,$J$=4) | | | | | |
| 15.4 | 245 ± 12 | 97 | 27.1 | 19.0 | 18.5 | 15.2 | 41.0 | 19.6 | 84.0 |
| 30.0 | 180 ± 8 | 87 | 30.8 | 22.3 | 18.2 | 20.0 | 52.2 | 25.7 | 90.9 |
| 45.0 | 128 ± 5 | 72 | 33.2 | 25.1 | 16.7 | 21.8 | 66.3 | 29.9 | 88.6 |
| | | | | Surface I: HF($v$=1,$J$=0) | | | | | |
| 15.4 | 495 ± 12 | 86 | 40.9 | 28.6 | 25.9 | 24.2 | 62.3 | 29.5 | 91.9 |
| 30.0 | 319 ± 9 | 75 | 41.5 | 30.1 | 23.3 | 26.2 | 79.0 | 35.2 | 93.0 |
| 45.0 | 234 ± 7 | 66 | 46.2 | 31.3 | 22.7 | 28.6 | 89.8 | 37.8 | 90.1 |
| | | | | Surface II: HF($v$=0,$J$=0) | | | | | |
| 3.8 | 1164 ± 22 | 88 | 21.9 | 16.4 | 12.5 | 12.7 | 35.7 | 17.2 | 90.5 |
| 9.6 | 589 ± 16 | 83 | 23.2 | 17.1 | 10.8 | 10.2 | 42.0 | 18.0 | 87.9 |
| 15.4 | 470 ± 12 | 75 | 24.2 | 17.4 | 11.2 | 13.4 | 46.2 | 19.4 | 87.1 |
| 20.0 | 382 ± 11 | 77 | 26.2 | 18.6 | 11.1 | 14.1 | 48.9 | 20.0 | 84.7 |
| 25.0 | 324 ± 10 | 66 | 26.4 | 18.1 | 8.7 | 13.0 | 56.2 | 20.2 | 85.1 |
| 30.0 | 265 ± 8 | 66 | 28.9 | 20.7 | 10.8 | 15.5 | 56.6 | 23.3 | 82.6 |
| 40.5 | 174 ± 7 | 58 | 32.1 | 23.0 | 9.6 | 15.4 | 65.1 | 25.1 | 86.5 |
| 45.0 | 154 ± 6 | 56 | 30.0 | 22.2 | 11.3 | 16.3 | 70.0 | 26.0 | 77.5 |
| 55.8 | 120 ± 6 | 58 | 36.0 | 26.7 | 15.4 | 21.1 | 70.7 | 31.9 | 75.7 |
| | | | | Surface IV: HF($v$=0,$J$=0) | | | | | |
| 3.8 | 905 ± 26 | 69 | 28.2 | 17.6 | 5.7 | 7.1 | 36.2 | 16.6 | 85.1 |
| 9.6 | 440 ± 16 | 67 | 28.6 | 18.8 | 5.4 | 7.3 | 41.9 | 17.9 | 82.2 |
| 15.4 | 351 ± 12 | 61 | 33.1 | 20.6 | 4.2 | 5.9 | 44.4 | 19.8 | 87.5 |
| 20.0 | 323 ± 11 | 54 | 29.9 | 19.2 | 4.1 | 6.9 | 52.2 | 19.0 | 82.3 |
| 25.0 | 241 ± 10 | 46 | 32.4 | 18.8 | 3.2 | 5.3 | 55.7 | 19.0 | 88.6 |
| 30.0 | 243 ± 8 | 40 | 33.8 | 22.3 | 3.5 | 7.5 | 59.1 | 22.6 | 86.7 |
| 40.5 | 156 ± 7 | 36 | 38.6 | 25.1 | 3.7 | 7.2 | 64.5 | 25.4 | 83.2 |
| 45.0 | 158 ± 6 | 36 | 37.4 | 23.8 | 3.8 | 8.1 | 70.1 | 24.3 | 81.0 |
| 55.8 | 140 ± 6 | 23 | 39.0 | 26.1 | 2.9 | 6.4 | 80.1 | 26.5 | 74.8 |

[a] $E_T$ = reactant translational energy (kJ/mol). [b] $\sigma$ = reaction cross section (bohr)$^2$; uncertainty is 1 standard deviation. [c] %$C$ = percent of reactive collisions which form complexes (more than one turning point in $\rho$). [d] $\langle\Delta E_{v'}\rangle$ = average vibrational energy in OH product (kJ/mol), not adjusted for zero-point energy. $\langle\Delta E_R\rangle$ = rotation; $\langle\Delta E_T\rangle$ = translation. [e] $\Delta$ = rms width of the corresponding distribution (kJ/mol). [f] $\langle\chi\rangle$ = average scattering angle (in degrees).

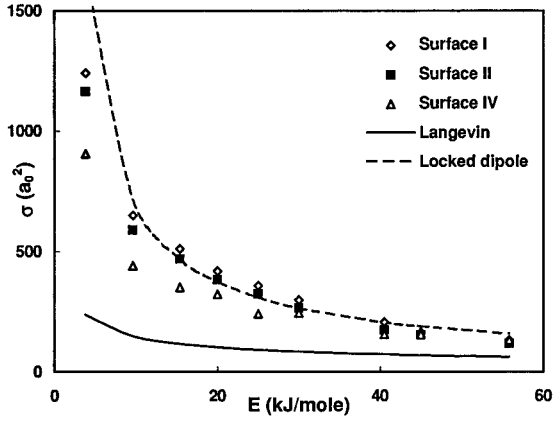


**Figure 3.** Total cross section for the reaction as a function of collision energy: 3D trajectory results (on three surfaces). The capture cross section for a locked dipole (ref 27) as well as the Langevin capture cross section are shown for comparison.

ranging from about 150$\hbar$ at 3.8 kJ/mol to about 260$\hbar$ at 55.8 kJ/mol. Opacity functions, $P(b)$, are generally flat, falling off only near $b_{max}$.

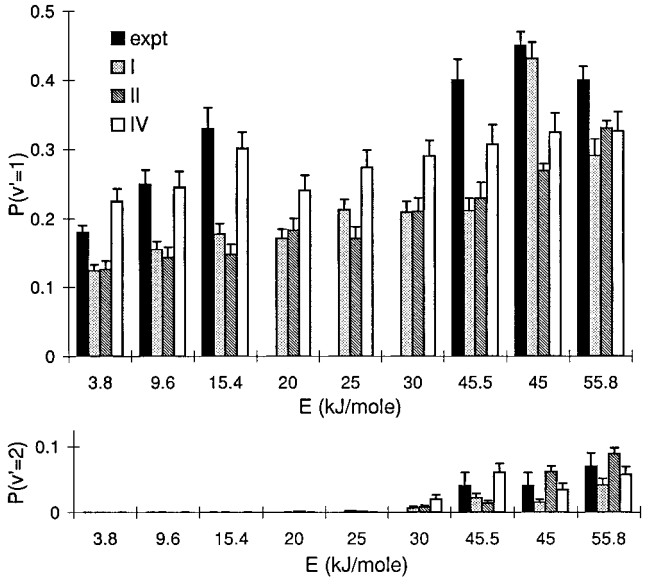


**Figure 4.** Probability of producing OH in $v' = 1$ and $v' = 2$: experiments (refs 6−8) and 3D trajectories on three surfaces. Error bars on the trajectory results represent 1 standard deviation in the statistics.

OH vibrational excitations are shown in Figure 4. There is a striking contrast between corresponding 1D and 3D results on the same surface: it is evident that the very strong preference for product vibrational excitation is an artifact of the collinear constraint. The 3D results are essentially the same for surfaces I and II, suggesting that when large impact parameter collisions have a major role, details of the shape of the corner of the surface are not important. However the shape of the bend does influence product vibration. At lower collision energies, the narrower bend of surface IV reduces the cross section while increasing vibrational excitation, in closer agreement with experiment. Surface IV also produces a significantly smaller fraction of complex collisions at all collision energies than surfaces I and II.

Surface I (and II which is similar) produces considerably more rotational excitation than surface IV. The amount of energy deposited in product rotation is fairly constant over the range of collision energies. Increased translation is converted into increased product vibration (∼25%) and translation (∼75%). Both the translational and rotational energy distributions are broad, as seen by the widths of the distributions in Table 3. The rotational distributions are not well-characterized by a single temperature. Given the large amounts of orbital angular momentum in these collisions, the amount of rotation in the products is surprisingly small: for surface IV the distributions peak at $J'$ values of 1 or 2, a bit higher for surfaces I and II. This is considerably less than that estimated in the crossed-beam experiments.[9]

A small study was made of the effect of internal excitation of HF, using surface I. Modest rotational excitation is relevant to the experiments, in which the target HF gas is thermal. Results are included in Table 3. The effects are not large. Excitation to $J = 4$ (4.9 kJ/mol) significantly decreases the total cross section, particularly at the lowest energies. A simple interpretation is that it is more difficult to orient a rotating molecule into a configuration favorable for reaction. Rotation also increases the probability of forming complexes. The added rotational energy emerges primarily as product rotation, with vibration increasing slightly. This result may explain, at least in part, the higher $J'$ values seen in the experiments.

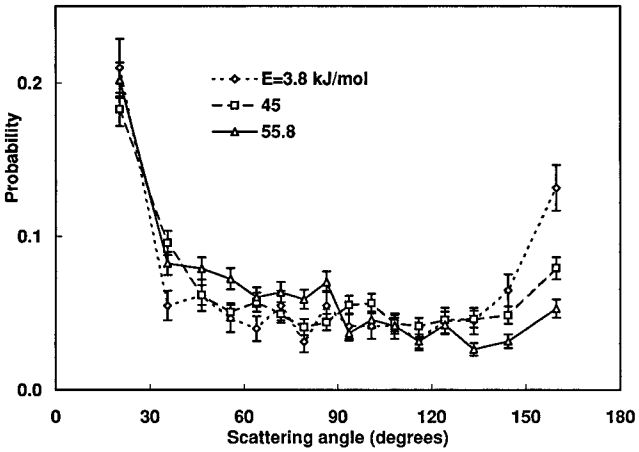


**Figure 5.** Angular distributions of the OH product for selected collision energies on surface IV. The angle $\chi$ is between the initial $O^-$ and final OH velocity vectors. The trajectories were binned in equal intervals of cos $\chi$. The distributions are normalized to unit area. Error bars represent 1 standard deviation in the Monte Carlo statistics.

Excitation of HF to $v = 1$ (47.4 kJ/mol added energy) appears to have little effect on the total cross section at lower collision energies but increases it a bit at higher energies, the vibrating molecule presenting a larger target. The amount of complex formation is little changed. The excess vibrational energy is distributed about 50% to translation, 30% to vibration, and 20% to rotation.

Sample angular distributions are shown in Figure 5. The scattering angle $\chi$ is measured between the velocity vectors of the reactant $O^-$ and the product OH. Histograms were collected in equal intervals of cos $\chi$, which would produce a flat distribution for isotropic scattering. There is distinct forward−backward peaking, as expected when complexes form with large orbital angular momentum. This is in qualitative accord with the crossed-beam experiments.[7,8] As the collision energy increases, all three surfaces exhibit some preference for forward scattering. This preference is particularly strong for direct collisions.

An intriguing result in the crossed-beam experiments[9] was the dependence of the angular distribution on the OH vibrational state. At 45.0 kJ/mol, OH $v = 0$ and 1 exhibit near forward−backward symmetry (with some overall preference for the forward hemisphere), while $v = 2$ favors forward scattering. At 55.8 kJ/mol all three show approximate forward−backward symmetry. We ran larger batches of trajectories on surface IV for these two energies, looking at the product vibrational state dependence of the angular distributions. Results are shown in Figure 6. Scattering in the forward hemisphere is somewhat preferred, more so at the higher energy. However, within the statistical uncertainty of the calculation (rather large for $v' = 2$ at the lower energy), there is no discernible vibrational state dependence of the angular distribution.

Because forward−backward peaking suggests long-lived collisions, Carpenter *et al.*[9] compared their results with statistical phase space theory.[28] At 45 kJ/mol, they found that the phase space vibrational distribution was somewhat colder than experiment, with less difference at 55.8 kJ/mol. They used a Langevin model to determine the maximum orbital angular momentum. Since our trajectory results imply that larger $L$ values are relevant, we repeated the phase space calculation with larger $L$'s. Despite an almost doubling of $L_{max}$, the results were essentially the same. Interestingly, the phase space predictions for the vibrational energy are closer to the trajectory results than to the experiment results. Yet the trajectory dynamics is not dominated by long-lived complexes.

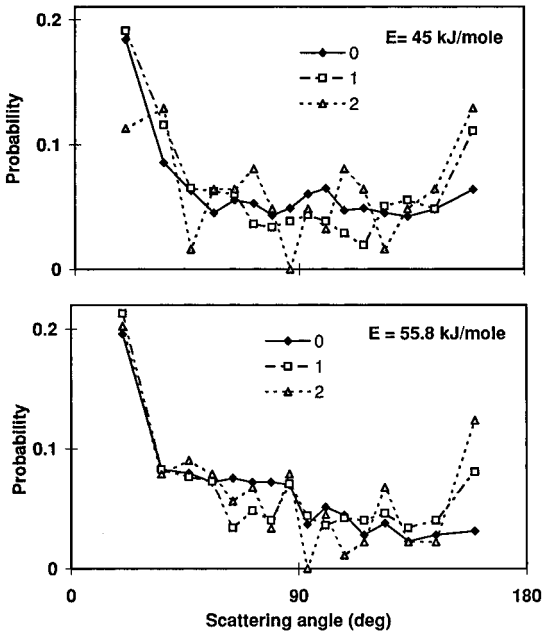


**Figure 6.** Angular distributions for surface IV at 45 and 55.8 kJ/mol, separated by the OH vibrational state. All are normalized to unit area. Statistical uncertainties for the $v' = 2$ product are rather large: the total number of trajectories constituting these distributions were 62 and 89, respectively.

There are some discrepancies between our trajectory results and the experiment results. No surface gives good agreement for the vibrational energy distributions at all energies. Details of the angular distribution differ, as discussed above. The trajectories appear to produce too little rotation with any of the surfaces, but particularly for surface IV. However, the observation of a rather strong dependence of product rotation on the steepness of the bend suggests that a better description of the off collinear region of the potential might remedy this.

Tachikawa, Takamura, and Yoshida[29] also carried out a 3D trajectory study of this system, using a LEPS surface with parameters based on their own *ab initio* calculations. The qualitative features of their surface in the strongly interacting region are similar to ours, although the LEPS function fails to produce the correct long-range behavior. They studied collision energies 5.01, 12.6, and 22.2 kJ/mol. As with our results, their $P(v'=1)$ results were slightly below Leone's, but exhibited similar trends. Like ours, their rotational distributions were not very sensitive to collision energy, and the broader part of the distribution peaks at $J' \approx 5$. However they observe a second (and larger) peak at $J' = 0$. They interpreted this as suggesting two competing mechanisms, one direct, producing a low $J'$, the other complex, producing a higher $J'$. On their LEPS surface, direct collisions preferentially produced vibrationally excited products. With our surfaces the opposite is true: the average vibrational energy in products is less for the direct reactive collisions.

Although we observed somewhat different contributions from direct and complex collisions, the distributions were not bimodal. In fact, the energy in product vibration was more strongly dependent on whether a collision began with a small or large impact parameter than on whether it was direct or complex. Figure 7 shows the 45 kJ/mol angular distribution again, but with contributions separated by intervals of impact parameter. The lowest parts of each bar correspond to the smallest impact parameter collisions: not surprisingly, they produce a nearly isotropic distribution. Since orbital angular momentum is relatively small in these close collisions, there is no forward−backward peaking. The second interval ($b^2$ from 32 to 64 $a_0^2$)

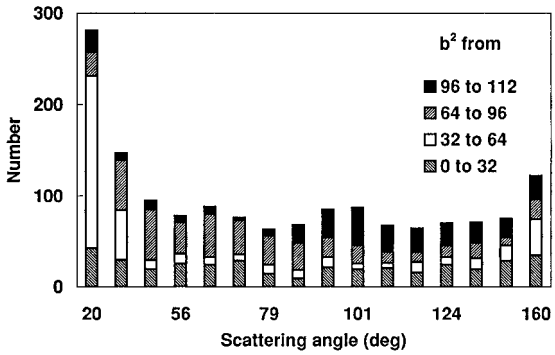


**Figure 7.** Angular distribution for surface IV at 45 kJ/mol, showing contributions from four statistically equal intervals of impact parameter *b* (in bohr). One thousand trajectories were run in each interval. The reaction probabilities in the four intervals are comparable (0.37, 0.41, 0.45, and 0.31).

is the major contributor to the strongly forward peak. These are the collisions which could be termed "spectator stripping". The third interval favors forward peaking somewhat but is more isotropic. It is the last interval which is surprising, showing a strong preference for the backward hemisphere. What is the mechanism? In these collisions, the $O^-$ ion, weakly trapped in the $OHF^-$ well, loops around HF like a boomerang, and extracts the proton as it flies back. Most of these large-impact parameter events are direct. Direct or complex, they produce OH with significantly lower vibrational and rotational excitation: at this energy, the average OH vibrational energy for all impact parameters is 34.7 kJ/mol, while the average in the largest interval of *b* is 23.2 kJ/mol.

## V. Conclusions

A frequent objective in detailed dynamical studies is a clearer understanding of the relationship between observed dynamical properties and the underlying forces, the potential energy surface. Beginning with the systematic studies by Polanyi and co-workers,[30] useful correlations have been found between energy disposal and the potential energy surface. Yet surfaces with deep wells are different: a much larger portion of configuration space is energetically accessible even at low collision energies. In the limit where the well produces very long-lived collisions, details of the potential become irrelevant and results are statistical.

Where does $O^- + HF$ fit into this picture? While a statistical model adequately describes some features, there is clear experimental evidence for nonstatistical behavior. Our trajectory results, along with those of Tachikawa *et al.*,[29] indicate that the vibrational distributions are fairly robust, not drastically sensitive to details of the potential. Rotation appears to be more sensitive to the potential. The shape of the bend, the noncollinear part of the potential, turns out to be quite important.

Are there important quantum effects which we have ignored? This is a special concern with light-atom transfer: the tight skew angle on the mass-weighted surface enhances the possibility of tunneling between the reactant and product valleys. However, for this system even at low collision energies the long-range attractive forces produce substantial kinetic energy in the reaction coordinate before the system reaches distances where tunneling would become important, so it is likely that this system behaves reasonably classically.

The potential energy surfaces used in this study are approximate. The fitting emphasized the well region, with very little information available elsewhere. In addition, we have treated this system with a single surface. Nevertheless, the trajectory studies give some insight into the role of the potential in the reaction dynamics.

**Acknowledgment.** S.C. acknowledges the generous hospitality of her hosts at the Laboratorio di Chimica Generale at the Università di Perugia, where the paper was written.

## References and Notes

(1) Squires, R. R.; Bierbaum, V. M.; Grabowski, J. J.; DePuy, C. H. *J. Am. Chem. Soc.* **1983**, *105*, 5185.

(2) Van Doren, J. M.; Barlow, S. E.; DePuy, C. H.; Bierbaum, V. M. *Int. J. Mass. Spectrom. Ion. Processes* **1991**, *109*, 305.

(3) Weisshaar, J.; Zwier, T. S.; Leone, S. R. *J. Chem. Phys.* **1981**, *75*, 4873.

(4) Langford, A. O.; Bierbaum, V. M.; Leone, S. R. *J. Chem. Phys.* **1985**, *83*, 3913.

(5) Hamilton, C. E.; Duncan, M. A.; Zwier, T. S.; Weisshaar, J. C.; Ellison, G. B.; Bierbaum, V. M.; Leone, S. R. *Chem. Phys. Lett.* **1983**, *94*, 4.

(6) Knutsen, K.; Bierbaum, V. M.; Leone, S. R. *J. Chem. Phys.* **1992**, *96*, 298.

(7) Levandier, D. J.; Varley, D. F.; Carpenter, M. A.; Farrar, J. M. *J. Chem. Phys.* **1993**, *99*, 148.

(8) Carpenter, M. A.; Zanni, M. T.; Levandier, D. J.; Varley, D. F.; Farrar, J. M. *Can. J. Chem.* **1994**, *72*, 828.

(9) Chapman, S. *Chem. Phys. Lett.* **1981**, *80*, 275.

(10) Kupperman, A.; Kaye, J. A.; Dwyer, J. P. *Chem. Phys. Lett.* **1980**, *74*, 257.

(11) Babamov, V. K.; Marcus, R. A. *J. Chem. Phys.* **1981**, *74*, 1790.

(12) Aquilanti, V.; Cavilli, S.; Laganà, A. *Chem. Phys. Lett.* **1982**, *82*, 179.

(13) Bondi, D. K.; Connor, J. N. L.; Manz, J.; Römelt, J. *Mol. Phys.* **1983**, *50*, 467.

(14) Hiller, C.; Manz, J.; Miller, W. H.; Römelt, J. *J. Chem. Phys.* **1983**, *78*, 3850.

(15) Manz, J.; Schor, H. H. H. *Chem. Phys. Lett.* **1984**, *107*, 549.

(16) Ali, D. P.; Hynes, J. T. In *Tunneling*; Jortner, J., Pullman, B., Eds.; Reidel: Dordrecht, The Netherlands, 1986; p 203.

(17) Chapman, S.; Ali, D. P.; Hynes, J. T. *Chem. Phys.* **1989**, *136*, 296.

(18) Skodje, R. *Ann. Rev. Phys. Chem.* **1993**, *44*, 145. A more complete bibliography on the theory of heavy−light−heavy dynamics is included in this review.

(19) Baer, M.; Last, I. *Chem. Phys. Lett.* **1985**, *119*, 393.

(20) Pollak, E.; Baer, M.; AbuSalbi, N.; Kouri, D. *Chem. Phys.* **1985**, *99*, 15.

(21) Persky, A.; Kornweitz, H. *J. Phys. Chem.* **1987**, *91*, 5496.

(22) Laganà, A.; Aguilar, A.; Gimenez, X.; Lucas, J. M. *Advances in Molecular Vibrations and Collision Dynamics*; JAI Press: Greenwich, CT, 1994; Vol. 2A, p 183.

(23) Bradforth, S. E.; Arnold, D. W.; Metz, R. B.; Weaver, A.; Neumark, D. *J. Phys. Chem.* **1991**, *95*, 8066.

(24) Bradforth, S. E.; Neumark, D. Private communication.

(25) Ellison, F. O. *J. Am. Chem. Soc.* **1963**, *85*, 3540. Tully, J. C. *Adv. Chem. Phys.* **1980**, *42*, 63.

(26) Kuntz, P. J.; Nemeth, E. M.; Polanyi, J. C.; Rosner, S. D.; Young, C. E. *J. Chem. Phys.* **1966**, *44*, 1168.

(27) Troe, J. State-Selected and State-to-State Ion-Molecule Reaction Dynamics, Part 2: Theory. *Adv. Chem. Phys.* **1992**, *82*, 485−529. See also Chesnavich, W. J.; Bowers, M. T. In *Gas Phase Ion Chemistry*; Bowers, M. T., Ed.; Academic Press: New York, 1978; Vol. 1, pp 119−151.

(28) Pechukas, P.; Light, J. C.; Rankin, C. *J. Chem. Phys.* **1966**, *44*, 3749.

(29) Tachikawa, H.; Takamura, H.; Yoshida, H. *J. Phys. Chem.* **1994**, *98*, 5298.

(30) Anlauf, K. G.; Polanyi, J. C.; Wong, W. H.; Woodall, K. B. *J. Chem. Phys.* **1968**, *49*, 5189. Maylotte, D. H.; Polanyi, J. C.; Woodall, K. B. *J. Chem. Phys.* **1972**, *57*, 1547. Parr, C. A.; Polanyi, J. C.; Wong, W. H. *J. Chem. Phys.* **1973**, *58*, 5.